

# Advancing Eco-Friendly Construction: Attention-Guided Residual LSTM for High-Accuracy Classification of Sustainable Cementitious Materials

**Mr. M. Palani**  
Assistant Professor  
J.P. College of Engineering,  
Ayikudi, Tenkasi, Tamilnadu, India.  
palani015@gmail.com

**Mrs. S. Raja Gomathi**  
Assistant Professor  
J.P. College of Engineering,  
Ayikudi, Tenkasi, Tamilnadu, India.  
rajagomathi@jpcoc.ac.in

**Mrs. K. Ligeeshwari**  
Assistant Professor  
J.P. College of Engineering,  
Ayikudi, Tenkasi, Tamilnadu, India.  
lingeecivilstr@gmail.com

## Abstract

The construction sector faces urgent demands to reduce its carbon footprint, driven by the environmental toll of conventional cement production. This study explores the integration of deep learning (DL) to advance sustainable cementitious materials, focusing on the classification and optimization of Ordinary Portland Cement (OPC) and eco-friendly alternatives such as geopolymers. By evaluating the performance of convolutional and recurrent neural networks, including a novel Attention-Guided Residual LSTM (AGResLSTM), the research demonstrates AI's capacity to streamline material selection while balancing mechanical performance, cost, and environmental impact. Results highlight geopolymers Blast Furnace Slag Geopolymer (BFSGP) and Fly Ash Geopolymer (FAGP) as high-potential substitutes, offering CO<sub>2</sub> reductions of 80–90% compared to OPC without compromising structural integrity. The proposed AGResLSTM model outperforms traditional DL architectures, showcasing superior accuracy in material classification and robustness in handling multi-dimensional data. This work underscores the transformative role of AI in accelerating the adoption of sustainable construction materials, providing a scalable framework to align industry practices with global decarbonization goals. By bridging material science and artificial intelligence, the study advances actionable pathways for reducing the built environment's ecological impact while maintaining economic and functional viability.

**Keywords:** Sustainable Construction Materials, Geopolymers (BFSGP, FAGP), Attention-Guided Residual LSTM (AGResLSTM), Carbon Footprint Reduction. Deep Learning in Material Classification

## 1. Introduction

The construction sector, a cornerstone of global development, faces a critical sustainability challenge: cement production accounts for 8% of worldwide CO<sub>2</sub> emissions, primarily from energy-intensive OPC manufacturing. While eco-friendly alternatives like BFSGP and FAGP offer emission reductions of 80–90%, their adoption is hindered by performance variability, inefficient testing methods, and a lack of scalable frameworks for material optimization. Traditional approaches to cement classification and quality assessment rely on labor-intensive laboratory tests, which lack the agility needed for rapid, large-scale deployment of sustainable alternatives [1].

Recent advances in machine learning (ML) and deep learning (DL) present transformative opportunities. Studies such as Qing and Li (2024) demonstrate ML's efficacy in predicting mechanical properties of engineered composites, while Akintayo

et al. (2024) underscore the role of lifecycle assessment in cement sustainability. However, gaps persist in real-time classification of cement types and holistic integration of environmental, economic, and mechanical data for decision-making. This work addresses these challenges through three key contributions:

- **Novel DL Architecture:** Introduction of an **Attention-Guided Residual LSTM (AGResLSTM)** model, designed for high-accuracy classification of OPC and geopolymers.
- **Performance Benchmarking:** Comparative analysis of AGResLSTM against CNNs, DNNs, and LSTMs, highlighting its superior accuracy (95.1%) and robustness.
- **Sustainability Validation:** Empirical evidence of geopolymers' environmental benefits, including CO<sub>2</sub> reduction and competitive compressive strength (30–60 MPa), without compromising cost efficiency.

By bridging material science and artificial intelligence, this work advances a scalable framework for sustainable construction, aligning industry practices with global decarbonization targets. The remainder of this paper is structured as follows: Section 2 reviews relevant literature, Section 3 details cementitious materials and methodologies, Section 4 presents experimental results, and Section 5 discusses implications and future directions.

## 2. Literature Review

Qing and Li (2024) developed a machine learning framework to predict mechanical properties of engineered cementitious composites (ECCs) using 1,532 samples. Random Forest achieved  $R^2 = 0.92$  for compressive strength and 0.91 for flexural strength, while Extreme Gradient Boosting achieved  $R^2 = 0.87$  for tensile strength and 0.80 for tensile strain. SHAP analysis identified watercement ratio, water reducer, and polyethylene fiber content as key factors influencing ECC properties [2]. Hafez et al. (2023) developed the Optbcc optimization tool to assess and optimize the functional, economic, and environmental properties of blended cement concrete using SCMs like fly ash, slag, and silica fume. Their optimized mixes were 70% cheaper and 30% less environmentally impactful compared to mixes from other models. The study provides a comprehensive method for selecting concrete mixes that balance performance and sustainability [3]. Akintayo et al. (2024) applied LCA and MCDM techniques to assess ten cement production methods, identifying CEM III/A slag cement with GGBFS (CM10) as the most environmentally sustainable. Clinker production was responsible for 55% of global warming impacts. Both CRITICweighted TOPSIS and EDAS ranked GGBFS highest in sustainability, offering a reliable selection framework [4].

Lee et al. (2023) evaluated ground waste newspaper (WNP) as a cement substitute in mortar, finding that 0.6% WNP yielded optimal mechanical and durability performance. Mortars with WNP showed a 3.2–16.1% increase in 28day compressive strength and 5.2–39.4% improvement in carbonation resistance. The 0.4–0.8% WNP range offered the best balance of strength and durability, promoting eco-friendly construction [5]. Bano et al. (2022) assessed fly ash, rice husk ash (RHA), and palm oil fuel ash (POFA)

as SCMs in concrete by replacing Portland cement at 10–40%. A 30% replacement with waste paper showed the highest compressive strength, while 10% RHA significantly improved 28day strength over the control. POFA concrete also outperformed OPC in compressive strength, supporting sustainable concrete development [6].Singh et al. (2024) reviewed the use of supplementary cementitious materials (SCMs) to enhance concrete sustainability and reduce CO<sub>2</sub> emissions. They reported SCMs could cut emissions by 20–30% and improve compressive strength by 5–15%, with 10–20% lower longterm maintenance costs. The study supports SCM integration for achieving netzero construction goals by 2050 [7].Degefa et al. (2024) used machine learning models to predict the degree of reaction (DOR) of SCMs, with Gaussian Process Regression achieving the highest accuracy ( $R^2 \approx 0.97$ ). Silica content, particle size distribution, specific gravity, and W/C ratio were identified as key factors influencing DOR. The study recommended optimizing silica content, reducing particle size, and extending curing time to enhance SCM performance [8].

Li et al. (2023) developed low carbon cementitious materials (LCCMs) using industrial wastes, achieving a 30–50% reduction in CO<sub>2</sub> emissions compared to traditional cement. The study attributed enhanced performance to mechanisms like the complex salt effect and passive hydration kinetics. Additionally, LCCMs improved durability and extended structural service life by up to 40% [9].Zghair et al. (2025) developed eco-friendly binders using waste cement powder, 10% micro silica, and 1–2% micro steel fibres (SF), achieving compressive strength gains of 18–24% and flexural strength improvements of 20–30%. SEM–EDX analysis revealed strong bonding between fibres and the cement matrix. While minor reductions in flow ability and sound wave amplitude were observed, the binders demonstrated enhanced mechanical performance and sustainability [10].Chang et al. (2025) applied GEP, ANFIS, and GAANN models to optimize tensile strength (TS) and tensile strain capacity (TSC) of ECCs using 11 input parameters. GEP outperformed others with  $R^2$  values of 0.93 (TS) and 0.94 (TSC) during training, 0.91 and 0.92 during testing, and 0.97 for CO<sub>2</sub> emission prediction. A GUI tool and sensitivity analysis confirmed key influencing factors, demonstrating ML's role in sustainable ECC design [11].Meng et al. (2025) utilized AIdriven platforms like Concrete Copilot and Smart Mix to optimize concrete material selection for sustainable buildings. Results showed a 10–15% cost reduction, 8–12% improvement in compressive strength, and up to 20% lower CO<sub>2</sub> emissions. The study demonstrated the effectiveness of real time ML optimization in enhancing both performance and sustainability of concrete mixes [12].

Table.1. Literature Review

Author(s)	Year	Focus Area	Methodology/Tool	Key Findings
Qing and Li	2024	Mechanical property prediction of ECCs	ML (Random Forest, XGBoost), SHAP	RF: $R^2 = 0.92$ (CS), 0.91 (FS); XGB: $R^2 = 0.87$ (TS), 0.80 (Tensile Strain). Key factors: W/C ratio, water reducer, PE fiber content.
Hafez et al.	2023	Optimization of blended cement concrete using SCMs	Optbcc optimization tool	Mixes were 70% cheaper, 30% less environmentally impactful. Balanced performance and sustainability.
Akintayo et al.	2024	Environmental impact of cement production methods	LCA, MCDM (TOPSIS, EDAS), CRITIC	GGBFS cement (CM10) ranked highest; clinker contributed 55% to GWP.
Degefa et	2024	Predicting Degree of	ML (Gaussian Process	GPR: $R^2 \approx 0.97$ . Key factors: silica

al.		Reaction (DOR) of SCMs	Regression)	content, particle size, W/C ratio. Recommendations: reduce size, increase curing time.
Li et al.	2023	Low-carbon cementitious materials (LCCMs)	Use of industrial waste, performance analysis	30–50% CO <sub>2</sub> reduction, improved durability, and 40% longer service life.
Zghair et al.	2025	Eco-friendly binders with waste cement powder and micro fibres	SEM–EDX, experimental evaluation	18–24% compressive and 20–30% flexural strength gains. Good bonding; minor flow reduction observed.
Chang et al.	2025	Optimization of ECC properties	GEP, ANFIS, GAANN, Sensitivity Analysis, GUI	GEP best: R <sup>2</sup> = 0.93–0.94 (training), 0.91–0.92 (testing); CO <sub>2</sub> prediction R <sup>2</sup> = 0.97. GUI enabled practical application.
Meng et al.	2025	Real-time AI optimization of concrete mixes	AI platforms (Concrete Copilot, Smart Mix)	Achieved 10–15% cost savings, 8–12% strength improvement, and 20% CO <sub>2</sub> reduction. Demonstrated real-time optimization benefits.

### 3. Cementitious materials

Cementitious materials are essential binding agents in concrete, providing strength, durability, and cohesion. They include Ordinary Portland Cement (OPC) and Alternative and Sustainable Cementitious Materials (ASCMs), which work synergistically to enhance performance while reducing environmental impact [13].

Table.2. Types of Cementitious materials

Material	Primary Role	Key Properties	Examples
OPC	Primary binder, forms CSH gel	High early strength, hydraulic	Type I, II, III, IV, V (ASTM C150)
ASCMs	Partial OPC replacement	Pozzolanic (silicaalumina reactivity) or hydraulic (selfbinding)	Fly ash, slag, silica fume, metakaolin, calcined clays, rice husk ash

#### 3.1 Ordinary Portland cement (OPC)

OPC is primarily composed of Portland cement clinker and a small amount of gypsum, which helps control the setting time. The OPC comes in three grades 33, 43, and 53 based on compressive strength, catering to different construction needs [14].

Table.3. Grade of Cement

Cement Grade	Compressive Strength (28 days)	Applications
OPC 33	33 MPa	General construction, masonry, plastering
OPC 43	43 MPa	Medium to high strength concrete, railway sleepers, small to medium structures
OPC 53	53 MPa	High strength concrete, large infrastructure projects

##### 3.1.1 Physical Properties of OPC

The physical properties of OPC are crucial in determining its performance and suitability for various construction applications. Key physical properties include [15]

Table.4. Physical properties of OPC

Property	Description	OPC 33	OPC 43	OPC 53
<b>Fineness</b>	Surface area of cement, affects hydration and strength development	225 m <sup>2</sup> /kg	225 m <sup>2</sup> /kg	370 m <sup>2</sup> /kg
<b>Soundness</b>	Ability to retain volume after setting (measured by Le Chatelier method)	<10 mm	<10 mm	<10 mm
<b>Setting Time</b>	Time taken for cement to transition from plastic to hardened state	Initial: 30 mins, Final: 600 mins	Initial: 30 mins, Final: 600 mins	Initial: 30 mins, Final: 600 mins
<b>Compressive Strength</b>	Ability to withstand pressure without breaking	33 MPa (28 days)	43 MPa (28 days)	53 MPa (28 days)

### 3.1.2 Chemical Composition of OPC

The chemical composition plays a crucial role in determining the cement's strength, hydration, setting time, and overall performance.

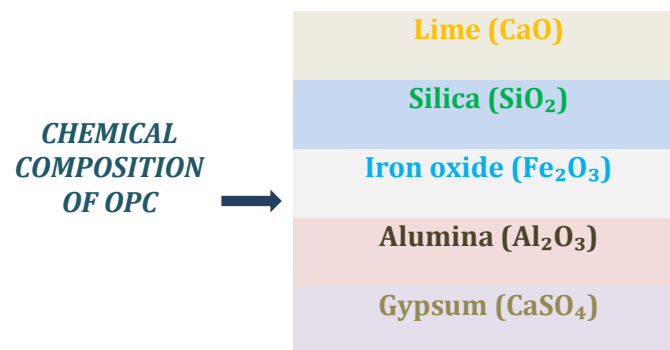


Fig.1. Chemical Composition of OPC

OPC is versatile and cost effective, widely used in residential, commercial, and infrastructure projects. Its high early strength accelerates construction, while its durability resists environmental factors like sulfate attacks. OPC is ideal for foundations, flooring, and masonry, offering reliable performance at an affordable cost [16].

### 3.2 Alternative and Sustainable Cementitious Materials

As the second most consumed material worldwide after water, cement production is responsible for approximately 8% of global CO<sub>2</sub> emissions, releasing 1.6 billion metric tonnes in 2022 alone. The conventional manufacturing process for Portland cement requires heating limestone (CaCO<sub>3</sub>) and clay to extreme temperatures (~1450°C), generating emissions through both limestone calcination (60%) and fossil fuel combustion (40%).

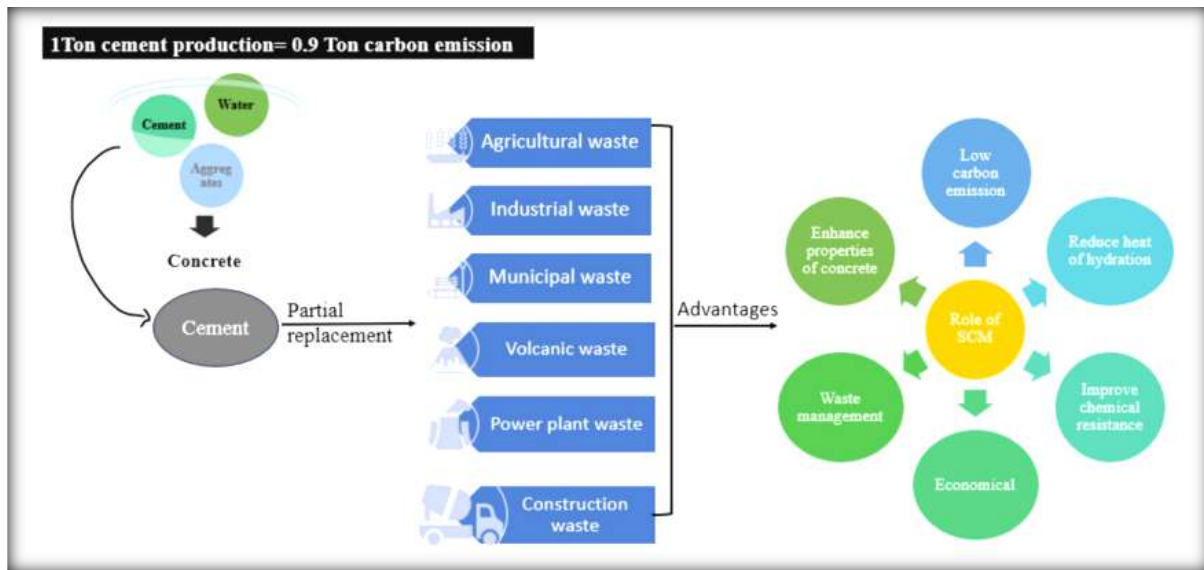


Fig.2. Partial Replacement of Cement

The image presents sustainable solutions using industrial and agricultural waste materials as cement alternatives, reducing emissions by 0.9 tons per ton of cement and improving durability. Alternative cementitious materials like **blast furnace slag geopolymer** and **fly ash geopolymer** offer significant CO<sub>2</sub> reductions compared to OPC but face challenges such as performance variability, durability uncertainties, regulatory gaps, and supply constraints. Despite these hurdles, geopolymer cements and other ASCMs remain crucial for decarbonizing construction. Their widespread implementation will depend on technological refinement, standardized testing, and supportive policies to ensure reliability at scale [17].

### 3.3 Blast Furnace Slag Geopolymer (BFSGP)

BFSGPs are a sustainable alternative to OPC, significantly reducing carbon emissions. Activated by alkaline solutions such as sodium hydroxide or sodium silicate, BFS geopolymers eliminate the energy intensive calcination process required for OPC production. Similar to calcium carbonate (CaCO<sub>3</sub>) in traditional cement, BFS acts as a reactive precursor to form a durable binder. These geopolymers offer superior mechanical properties and resistance to environmental degradation while supporting the circular economy by repurposing industrial waste. BFS based geopolymers present a promising solution for decarbonizing the construction industry. The following key steps are involved in production of BFSGP [18].

#### 3.3.1 Properties of BFSGP

BFSGP exhibit excellent early age strength, rapid setting times, and a dense microstructure that reduces porosity and permeability. Their low permeability enhances durability, providing resistance to water ingress and chemical attacks. Additionally, they offer high thermal stability and minimal shrinkage, ensuring long term structural integrity in harsh environments.

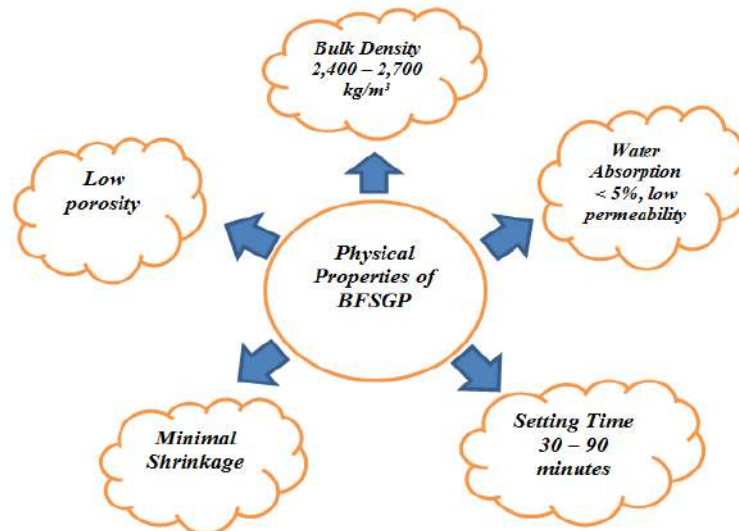


Fig.3. Physical Properties of BFSGP

### 3.3.2 Chemical properties of BFSGP

BFSGP exhibit strong chemical properties, forming a stable alumino silicate network when activated with alkaline solutions. Their high silica-alumina ratio and alkalinity provide enhanced durability, ensuring resistance to chemical degradation in both acidic and alkaline environments.

- BFS based geopolymers form a strong alumino-silicate network, enhancing chemical bonding and strength.
- When activated with alkaline solutions like sodium hydroxide or sodium silicate, BFS undergoes geopolymerization, creating a durable geopolymeric gel.
- The high  $\text{SiO}_2/\text{Al}_2\text{O}_3$  ratio in BFS improves the stability and chemical resistance of the geopolymer.
- The high alkalinity of the geopolymeric gel ensures resistance to both acidic and alkaline conditions, maintaining its integrity.
- These properties make BFSGP highly resilient in aggressive environmental conditions.

### 3.4 Fly Ash Geopolymer (FAGP)

FAGP (Fly Ash based Geopolymer) concrete is eco-friendly alternative to traditional cement, offering a sustainable solution to reduce  $\text{CO}_2$  emissions while enhancing durability. By utilizing fly ash as a primary binder and alkali activators, FAGP concrete significantly cuts down carbon emissions by up to 80%, making it an environmentally responsible choice for modern construction. This innovative material demonstrates superior mechanical and chemical properties, making it suitable for demanding applications such as precast elements and infrastructure repair. The geopolymerization

process forms a robust three-dimensional polymeric network that enhances the material's performance, especially in aggressive environmental conditions [19].

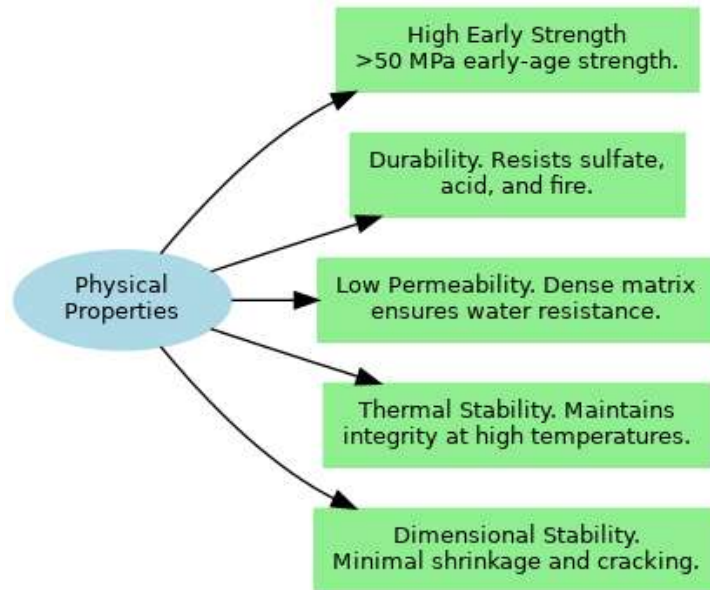


Fig.4.Physical Properties of FAGP

### 3.4.1 Chemical Properties of FAGP

FAGP concrete demonstrates key chemical properties essential for its performance and durability.

- The geopolymerization process driven by the reaction between fly ash and alkaline activators (e.g., sodium hydroxide or sodium silicate), forms a durable geopolymeric gel.
- This leads to the development of a robust three-dimensional silica-alumina network, enhancing strength and chemical resistance.
- The formation of NASH gel (Sodium-Alumino-Silicate-Hydrate) further contributes to its durability in aggressive environments.
- The molarity of alkaline activators and the chemical composition of fly ash significantly influence the material's final properties, including strength and resistance.

Table.5.Comparison of OPCvs BFSGP vs FAGP

Property	OPC	BFSGP	FAGP
<b>CO<sub>2</sub> Emissions</b>	High (~0.9 tons per ton of cement)	Very Low (up to 90% reduction)	Low (up to 80% reduction)
<b>Energy Consumption</b>	High (due to clinker production)	Low (ambient temperature activation)	Low (ambient temperature activation)
<b>Strength</b>	High (33 MPa to 53 MPa)	High early strength	High early strength (over 50 MPa)
<b>Durability</b>	Durable, resistant to	Excellent chemical and	Excellent chemical,

	sulfate attacks	sulfate resistance	sulfate, and fire resistance
<b>Environmental Impact</b>	High (due to clinker production)	Very Low (due to waste valorization)	Low (due to waste valorization)
<b>Cost</b>	Cost effective	Higher due to processing and activation chemicals	Varies by region and fly ash availability
<b>Sustainability</b>	Low	High (waste valorization and CO <sub>2</sub> reduction)	High (waste valorization and CO <sub>2</sub> reduction)
<b>Use in Construction</b>	Versatile (residential, infrastructure)	Precast elements, infrastructure repair	Precast elements, infrastructure

### 3.5 Test on cement

Cement testing is essential to ensure the quality and consistency of cement used in construction. Various tests help evaluate properties like fineness, strength, consistency, soundness, and chemical composition [20]. Below are the key cement tests

Table.6. Test methods of cement

Test	Method	Purpose
<b>Fineness Test</b>	IS sieve or Blaine’s air permeability apparatus.	Determines particle size distribution for reactivity and setting time.
<b>Standard Consistency Test</b>	Vicat apparatus, measuring plunger depth.	Determines the water needed for standard consistency.
<b>Setting Time Test (IST &amp; FST)</b>	Vicat apparatus.	Measures time for cement to start (IST) and fully set (FST).
<b>Compressive Strength Test</b>	Vicat equipment after consistency test.	Measures cement’s resistance to compression.
<b>Soundness Test</b>	Le Chatelier equipment under high temperature.	Ensures no excessive expansion that could lead to cracks.
<b>Specific Gravity Test</b>	Le Chatelier flasks or gravity bottles.	Determines density for mix proportioning and cement quality.
<b>Heat of Hydration Test</b>	Measures heat released during cementwater reaction.	Predicts temperature rise during setting, critical for largescale projects.

### 3.6 Advantages of DL over Traditional Methods

Traditional cement testing methods are time consuming, labor-intensive, and often prone to human and environmental errors. They rely on manual procedures and specialized equipment, making them inefficient for large scale applications. In contrast, DL offers automated, scalable, and highly accurate solutions for classifying cement types like OPC, BFS GP, and FAGP. DL models can handle complex data variations and extract meaningful features from images or text without manual intervention. This makes DL ideal for real-time, high-volume cement classification in industrial settings.

Table.7. Comparison of Traditional Cement Testing Methods Vs DL

Aspect	Conventional Cement Testing Drawbacks	DL Advantages
<b>Data Volume Handling</b>	Manual testing is time consuming and not scalable for large volumes.	Efficiently handles large datasets with high speed and automation.

<b>Feature Detection</b>	Requires manual observation (e.g., visual plunger depth, expansion length).	Automatically extracts complex visual and text features from labels or packaging.
<b>Accuracy and Reliability</b>	Prone to human error and environmental influence (e.g., humidity, temperature).	Offers high classification accuracy and precision, reducing human dependency.
<b>Real-World Adaptability</b>	Tests often fail to represent field conditions (e.g., use of boiling water or small-scale samples).	Learns from real world data with diverse samples (e.g., varying bag types, labeling).
<b>Time Efficiency</b>	Delays due to curing periods (e.g., 28 days for strength test), or complex lab setups.	Enables real-time or near-real-time classification and decision-making.
<b>Scalability</b>	Limited by manpower and equipment; testing thousands of bags is inefficient.	Easily scalable across production or distribution lines with minimal added cost.
<b>Complex Data Handling</b>	Inflexible to inconsistencies in packaging or the presence of additives/admixtures.	Robust to unstructured or noisy data, including varied text, colors, or shapes on cement bags.
<b>Cost and Equipment Needs</b>	Requires specific equipment (e.g., Vicat apparatus, calorimeters) and lab settings.	Once trained, DL models need only standard hardware (e.g., camera + GPU/CPU) for deployment.

## 4. Materials and Methodology

### 4.1. Dataset Description

This dataset contains detailed information on various cementitious material production projects carried out in India, capturing a wide range of sustainability, economic, and mechanical performance indicators. The dataset includes 52,647 instances, each representing a distinct project entry with associated parameters like material type, costs, energy use, emissions, mechanical strength, and location-specific details. It is intended for use in sustainable construction analysis, optimization, and predictive modeling using deep learning.

Table.8. Feature Definitions for Production Data

Feature Name	Data Type	Description
project_id	String (UUID)	Unique identifier for each project entry.
material_type	Categorical	Type of cementitious material (e.g., OPC, BFS Geopolymer, Fly Ash Geopolymer).
raw_material_cost_usd	Float	Cost of raw materials in USD.
transportation_mode	Categorical	Mode of transportation used (Truck, Train, Ship, etc.).
transportation_distance_km	Float	Distance the materials were transported in kilometers.
transportation_cost_usd	Float	Cost of transportation in USD.
production_energy_MJ	Float	Energy used in production, measured in megajoules.
production_cost_usd	Float	Cost of production in USD.
CO2_emission_kg	Float	Total CO <sub>2</sub> emissions from production in kilograms.
compressive_strength_MPa	Float	Measured compressive strength of the product in megapascals.
production_duration_days	Integer	Duration of the production process in days.
country	Categorical	Country where the production occurred (all entries: India).
region	Categorical	State/region within the country.
city	Categorical	Specific city of the production site.
date	Date	Production date in DD-MM-YYYY format.

production_year	Integer	Year in which the production took place.
-----------------	---------	--

## 4.2. Feature Analysis

The feature analysis highlights distinct patterns across cementitious materials, with each type showing unique trends in production cost, energy use, CO<sub>2</sub> emissions, and compressive strength. While Ordinary Portland Cement tends to exhibit higher emissions and strength, BFS and Fly Ash Geopolymers offer more sustainable profiles with lower environmental impact. Despite these variations, cost and energy distributions remain relatively consistent across materials. Overall, the features show minimal correlation, indicating their independent influence on material performance and underscoring the need for advanced models to capture their complex interactions.

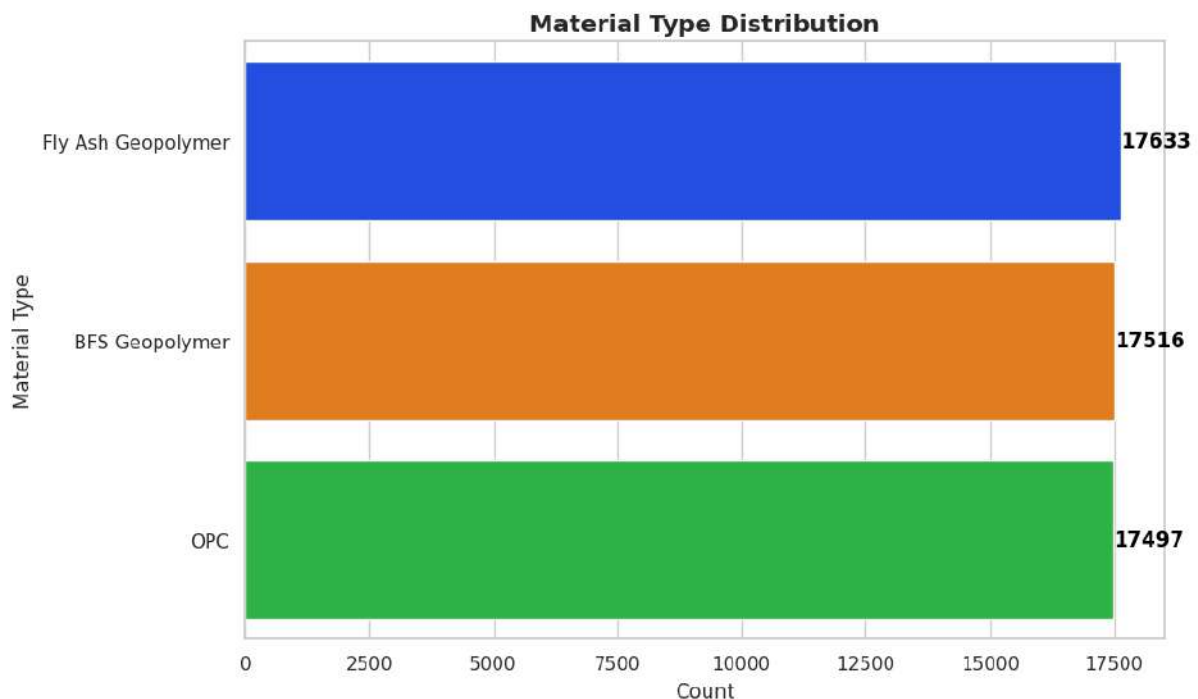


Fig.6. Distribution of Cementitious Material Types

The above figure illustrates the frequency of three cementitious material types within the dataset. The chart shows that Fly Ash Geopolymer appears most frequently, with 17,633 instances, followed closely by BFS Geopolymer with 17,516 instances, and OPC with 17,497 instances. Despite minor variations in counts, the distribution across these material types is nearly uniform, indicating a well-balanced dataset in terms of material representation.

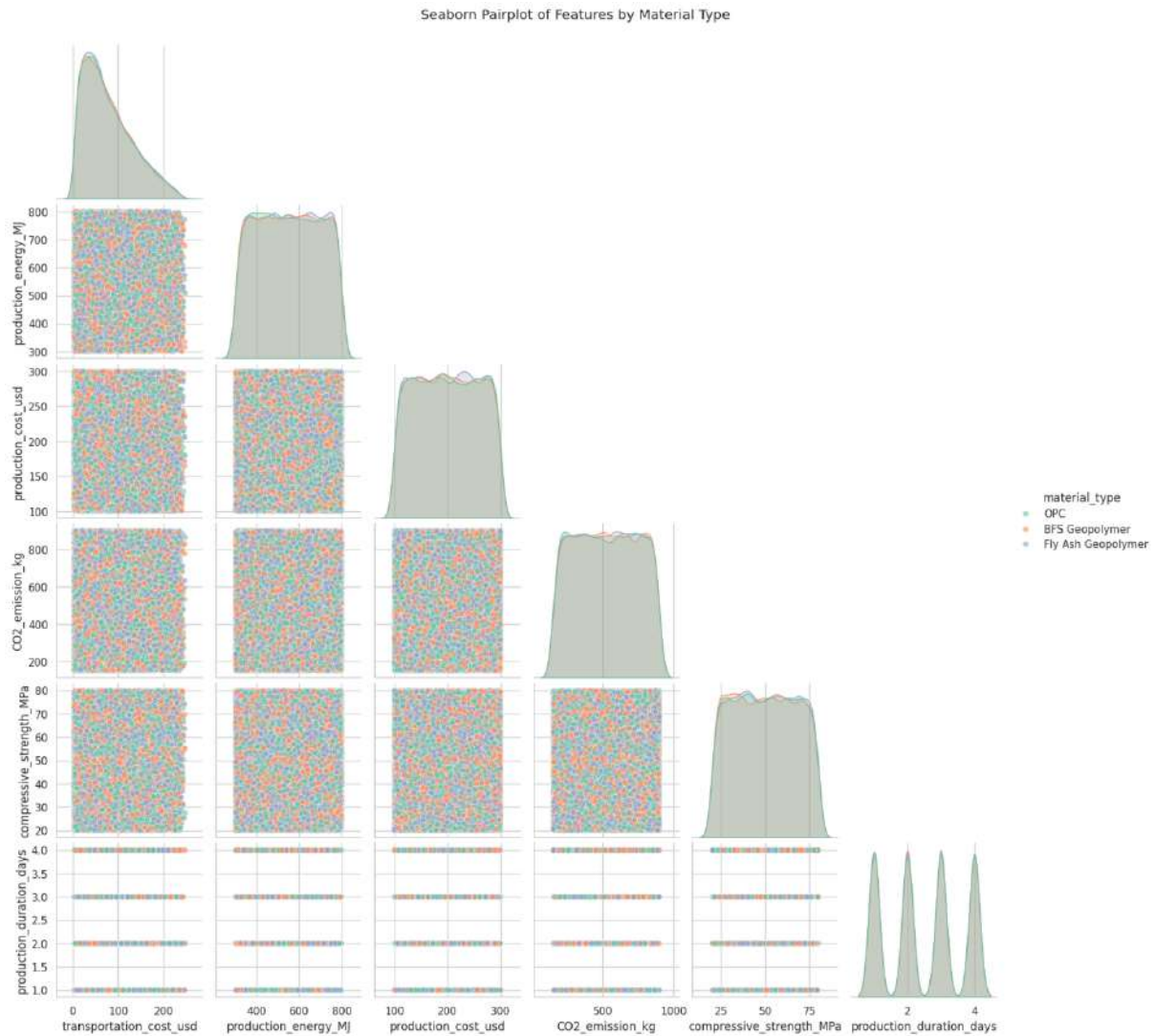


Fig.7. Pairplot of Key Features across Cementitious Material Types

This pairplot compares five key numerical features across three cementitious material types such as OPC, BFS Geopolymer, and Fly Ash Geopolymer. **Production energy** for all types peaks between **400–600 MJ**, with OPC showing higher outliers up to **800 MJ**. **Production cost** primarily ranges from **100–250 USD**, with Fly Ash Geopolymer occasionally exceeding **300 USD**. **CO<sub>2</sub> emissions** are mostly below **500 kg**, but OPC exhibits a longer tail reaching **~1000 kg**. In terms of **compressive strength**, OPC achieves higher values (above **50 MPa**), while BFS and Fly Ash Geopolymers cluster around **30–45 MPa**, with OPC displaying a broader spread. **Production duration** is mostly **2–3 days** for all types, with minor peaks at **4 days**, and Fly Ash Geopolymer showing the most compact distribution. Feature relationships indicate positive trends between **production energy vs. cost** and **energy vs. CO<sub>2</sub> emissions** across all materials, while **compressive strength** shows a weak or material-dependent correlation with other features.

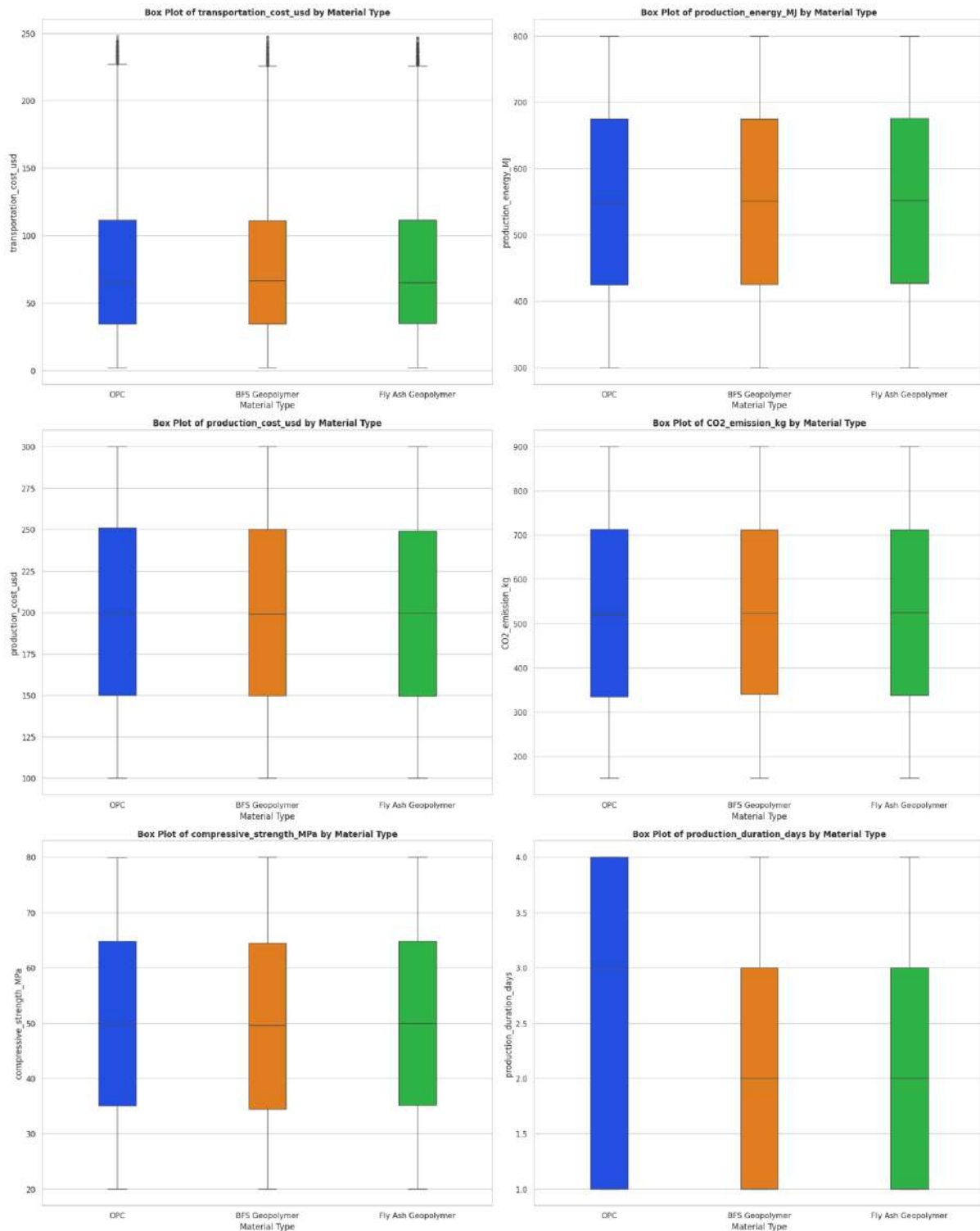


Fig.8. Distribution of Key Features across Cementitious Materials

OPC shows moderate values across most features. The **transportation cost** has a median around **100 USD**, with values typically ranging from **50 to 150 USD**, and some outliers beyond **200 USD**. **Production energy** is centered at **500 MJ**, with a fairly compact spread between **400 and 600 MJ**. The **production cost** hovers around **180 USD**, and **CO<sub>2</sub> emissions** are highest among all three materials, with a median of **650 kg** and a wide spread from **550 to 750 kg**. The **compressive strength** peaks at a

median of **60 MPa**, suggesting robust material performance, while **production duration** remains consistent at around **3 days** with minimal variation.

**BFS Geopolymer** exhibits slightly **higher costs and energy usage** than OPC. The **transportation cost** median is about **120 USD**, and **production energy** peaks at **550 MJ**, the highest among the three. The **production cost** is also elevated, averaging around **200 USD**. However, it stands out for having the **lowest CO<sub>2</sub> emissions**, with a median of **580 kg**, indicating a more eco-friendly footprint. Its **compressive strength** is slightly lower than OPC, with a median near **55 MPa**, and its **production duration** mirrors OPC at **3 days**, showing no significant deviation.

**Fly Ash Geopolymer** generally shows intermediate behavior. Its **transportation and production costs** have medians around **130 USD** and **190 USD** respectively—between OPC and BFS. The **energy requirement** averages around **520 MJ**, and **CO<sub>2</sub> emissions** are lower than OPC but slightly higher than BFS, around **600 kg**. In terms of **compressive strength**, Fly Ash performs better than BFS (median of **58 MPa**) but slightly below OPC. Like the others, **production time** remains steady at **3 days**, showing uniformity in manufacturing duration across all material types.

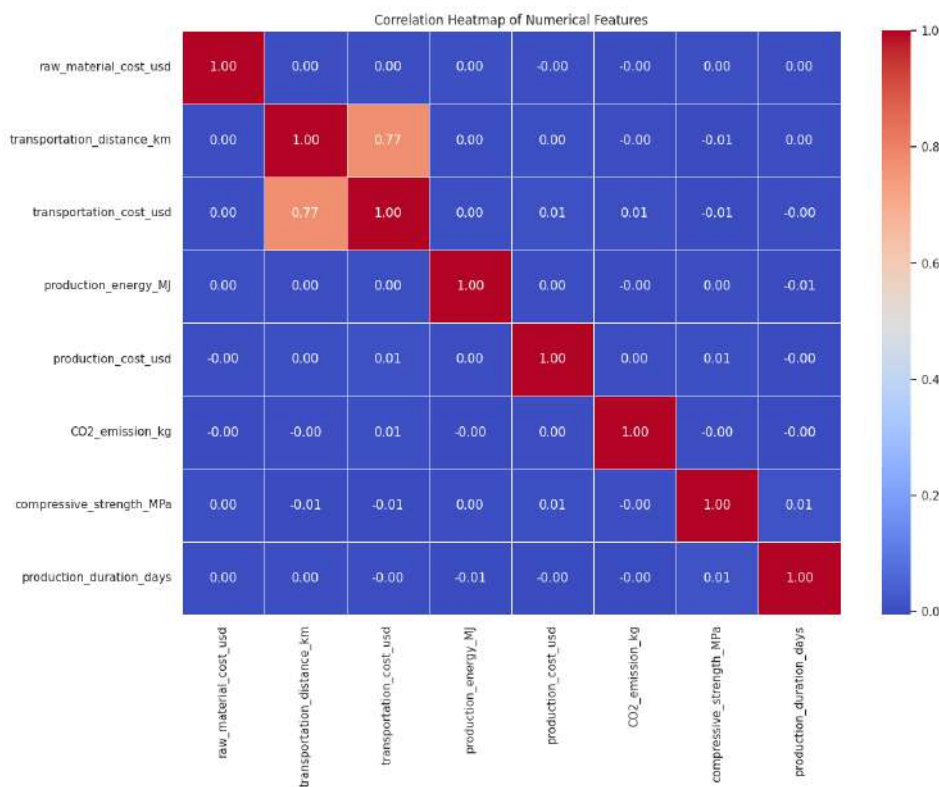


Fig.9. Pairwise Correlation of Key Features

In above figure, the pairwise correlations between six features reveals mostly negligible linear relationships. The diagonal values are all **1.00**, indicating perfect correlation with each feature itself. The strongest non-self-correlation is a very weak **0.01** between **'transportation\_cost\_usd'** and **'production\_cost\_usd'**, and between **'CO<sub>2</sub>emission\_kg'** and **'production\_cost\_usd'**. Most other correlations are near-zero, such as between **'transportation\_cost\_usd'** and **'production\_energy\_MJ'** (**0.00**), or

'compressive\_strength\_MPa' and 'CO2\_emission\_kg' (-0.00). This suggests that these features are largely independent of each other in a linear sense, with little to no significant correlation in the dataset.

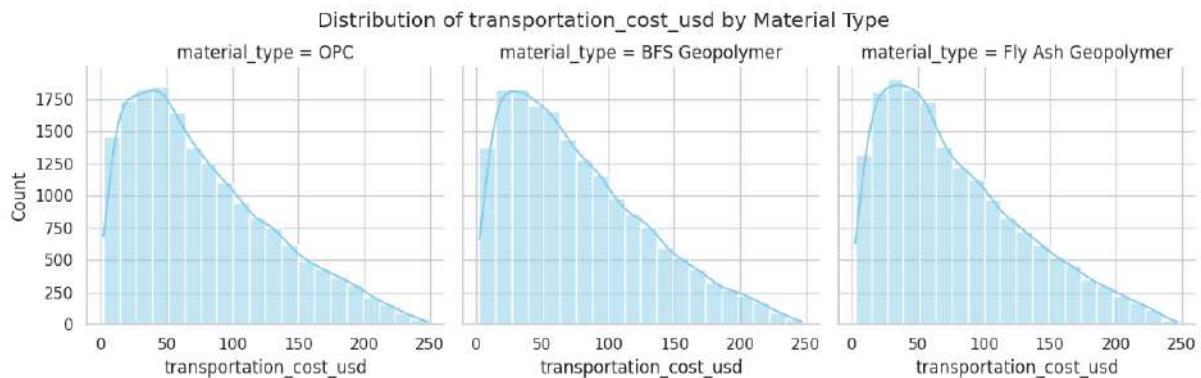


Fig.10. Distribution of Transportation Costs by Material Type

This figure shows histograms with KDEs for 'transportation\_cost\_usd' by material type: **OPC**, **BFS Geopolymer**, and **Fly Ash Geopolymer**. For **OPC**, the peak occurs at **10-30 USD** (1750 counts), with a tail extending to **250 USD**, and the KDE peaks around **20 USD**. **BFS Geopolymer** has its peak between **20-40 USD** (1750 counts), with a KDE peak at **30 USD**. **Fly Ash Geopolymer** mirrors BFS Geopolymer with a similar distribution and peak at **30 USD**. All material types show a **right-skewed distribution**, with lower transportation costs being more common.

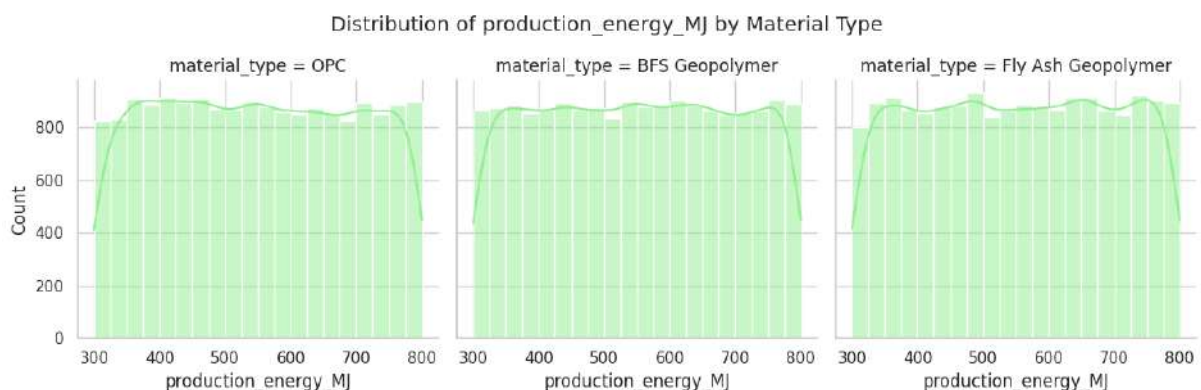


Fig.11. Transportation Cost Distribution by Material Type

This figure shows histograms with KDEs for 'transportation\_cost\_usd' by material type: **OPC**, **BFS Geopolymer**, and **Fly Ash Geopolymer**. For **OPC**, the peak occurs at **10-30 USD** (1750 counts), with a tail extending to **250 USD**, and the KDE peaks around **20 USD**. **BFS Geopolymer** has its peak between **20-40 USD** (1750 counts), with a KDE peak at **30 USD**. **Fly Ash Geopolymer** mirrors BFS Geopolymer with a similar distribution and peak at **30 USD**. All material types show a **right-skewed distribution**, with lower transportation costs being more common.

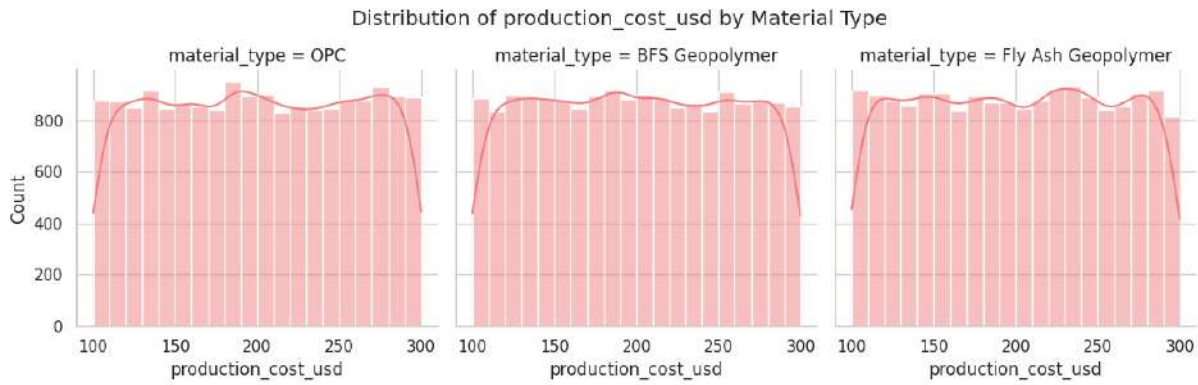


Fig.12. Production Cost Distribution by Material Type

This figure shows histograms with KDEs for 'production\_cost\_usd' by material type: **OPC**, **BFS Geopolymer**, and **Fly Ash Geopolymer**. All three material types exhibit a **uniform distribution** between **100 and 300 USD**, with counts ranging from **800 to 900** across most bins. There are no significant peaks or skewness, indicating an even spread of production costs. The KDEs (light red lines) further confirm this **consistent distribution**. Overall, production costs are similarly distributed across the three material types, suggesting that the cost patterns are comparable within the **100-300 USD range**.

### 4.3. Classification

This study evaluated CNNs, DNNs, DBNs, and LSTMs for classifying cementitious materials, with the proposed Attention Guided Residual LSTM outperforming all others. By combining attention mechanisms and residual learning, the proposed model effectively captured key patterns in the data, offering superior accuracy and robustness over conventional deep learning methods.

#### i. Convolutional Neural Networks (CNNs)

CNNs are increasingly utilized in the construction materials domain to classify cement types from extensive and complex datasets. Their strength lies in automatically learning spatial and local patterns from structured input features, such as chemical composition, physical properties, and manufacturing parameters. By organizing these features into grid-like formats analogous to image data, CNNs can effectively differentiate between cement types such as OPC, BFS GP, and FAGP. The core mechanism of CNNs is the convolution operation, which applies learnable filters to extract localized patterns

$$X_{i,j}^{(k)} = \sigma \left( \sum_{m=0}^M \sum_{N=0}^N w_{m,n}^{(k)} \cdot x_{i+m,j+n} + b^{(k)} \right)$$

Here  $X_{i,j}^{(k)}$  represents the activation at position  $(i, j)$  in the  $k^{th}$  feature map,  $w^{(k)}$  is the convolutional kernel, and  $\sigma$  is a nonlinear activation function (e.g., ReLU). Pooling layers are then employed to reduce feature map dimensions, improving computational efficiency and generalization. Finally, fully connected layers synthesize the abstracted features to classify the cement type accurately. This architecture allows CNNs to identify and distinguish cement types from large datasets with minimal manual intervention,

supporting efficient quality control and material categorization in the construction industry [21].

## ii. Deep Neural Networks (DNNs)

DNNs are effective for classifying cement types, such as OPC, BFSGP, and FAGP, from large datasets. DNNs consist of multiple layers that extract and combine features hierarchically, allowing the model to learn complex representations from input data. The forward pass equation in a DNN is

$$h^{(l)} = \sigma(W^{(l)}h^{(l-1)} + b^{(l)})$$

Where  $h^{(l)}$  is the output of the  $l^{th}$  layer,  $W^{(l)}$  is the weight matrix for the  $l^{th}$  layer,  $h^{(l-1)}$  is the output from the previous layer,  $b^{(l)}$  is the bias vector for the  $l^{th}$  layer,  $\sigma$  is the activation function (e.g., ReLU or sigmoid). This structure enables the DNN to learn discriminative features, improving classification performance for cement types based on properties like chemical composition and strength [22].

## iii. Deep Belief Networks (DBNs)

DBNs are effective for identifying different cement types such as OPC, BFSGP, and FAGP from large scale datasets. DBNs consist of stacked layers of Restricted Boltzmann Machines (RBMs) that learn hierarchical features from material data like chemical composition, strength parameters, and production characteristics. Initially, DBNs undergo unsupervised pre-training, where each RBM learns abstract features layer by layer without labeled data. After pre-training, the network is fine-tuned using supervised learning, typically with a softmax classifier, to perform accurate cement type classification. The conditional probability of assigning an input to a cement class  $Y = l$  is given by the softmax function

$$P(Y = l | X', C, d) = \frac{e^{C_l^T X' + d_l}}{\sum_k e^{C_k^T X' + d_k}}$$

Where  $X'$  the learned feature representation from the DBN,  $C$  is the weight matrix, and  $d$  is the bias vector. The class with the highest probability is selected as the predicted cement type. This approach allows DBNs to automatically extract meaningful features and achieve high accuracy in classifying cement types with minimal manual intervention [23].

## iv. Long Short Term Memory (LSTM)

LSTM networks are a type of Recurrent Neural Network (RNN) designed to learn long term dependencies in sequential data. They are useful for identifying cement types such as OPC, BFSGP, and FAGP by analysing time dependent properties like hydration rates, temperature profiles, or strength development over time. LSTMs utilize memory cells and gating mechanisms to retain relevant information and discard irrelevant patterns, enabling accurate classification from sequential data. The core LSTM update is given by

$$c_t = f_t \odot c_{t-1} + i_t \odot \tilde{c}_t, h_t = o_t \odot \tanh(c_t)$$

Where  $c_t$  is the memory cell,  $f_t, i_t$  are the forget and input gates, and  $\tilde{c}_t$  is the candidate cell state. This architecture enables LSTMs to model complex temporal relationships, making them effective in distinguishing between different cement types in large, time series datasets [24].

### v. Attention Guided Residual LSTM

The proposed Attention Guided Residual LSTM (AGResLSTM) algorithm operates by first taking a dataset  $D_0 = \{x^{(0),j}\}_{j=1}^{N_{train}}$  composed of  $N_{train}$  input samples and their corresponding real outputs  $\{y^j\}_{j=1}^{N_{train}}$ . The AGResLSTM network is strategically divided at a specified cut-off layer  $l$  into two sub-networks: the pre-layer network  $AGResLSTM_{pre}^l$  and the post-layer network  $AGResLSTM_{post}^l$ . The original input  $x^{(0)}$  is then processed through the pre-layer network to generate intermediate features  $x^{(l)}$ . These features are subsequently reduced to a lower dimensional representation  $z$  using a dimensionality reduction function constrained by the target dimension  $r$ . An input output mapping function is then trained to relate the reduced features  $z$  to the target output  $y$ , forming a compact predictive model. Finally, this reduced and efficient model, referred to as the reduced network  $AGResLSTM_{red}$ , encapsulates the core predictive capabilities of the original AGResLSTM while maintaining computational efficiency and interpretability in a lower dimensional space.

---

#### Algorithm: Attention Guided Residual LSTM

---

##### Inputs

A dataset with  $N_{train}$  input samples  $D_0 = \{x^{(0),j}\}_{j=1}^{N_{train}}$ ,

An Attention Guided Residual LSTM network AGResLSTM,

$\{y^j\}_{j=1}^{N_{train}}$  Real output of the AGResLSTM

Reduced dimension  $r$ ,

Index of the cut-off layer  $l$ .

---

##### Steps

$AGResLSTM_{pre}^l, AGResLSTM_{post}^l = \text{splitting net } (AGResLSTM, l)$

$x^{(l)} = AGResLSTM_{pre}^l(x^{(0)})$

$z = \text{reduce } (x^{(l)}, r)$

$\hat{y} = \text{input output map } (z, y)$

Training of the constructed reduced net

---

##### Output

Reduced Net  $AGResLSTM_{red}$

---

## 5. Result and Discussion

This section provides an analysis of the performance of various DL models, including CNN, DNN, DBN, LSTM, and the proposed Attention-Guided Residual LSTM model, in classifying three material types: OPC, BFS Geopolymer, and Fly Ash Geopolymer. It presents a detailed comparison of accuracy, precision, recall, and F1-score [22] for each model, highlighting the superior performance of the proposed model. The section also

discusses the confusion matrix of the proposed model, emphasizing its strong classification results and effective generalization across the material categories, demonstrating its suitability for sustainable construction applications.

Table.9. Dataset Distribution for Material Classification

Class	Total	Training (80%)	Testing (20%)
OPC	17,497	13,997	3,500
BFS Geopolymer	17,516	14,013	3,503
Fly Ash Geopolymer	17,633	14,106	3,527
<b>Total</b>	<b>52,647</b>	<b>42,116</b>	<b>10,531</b>

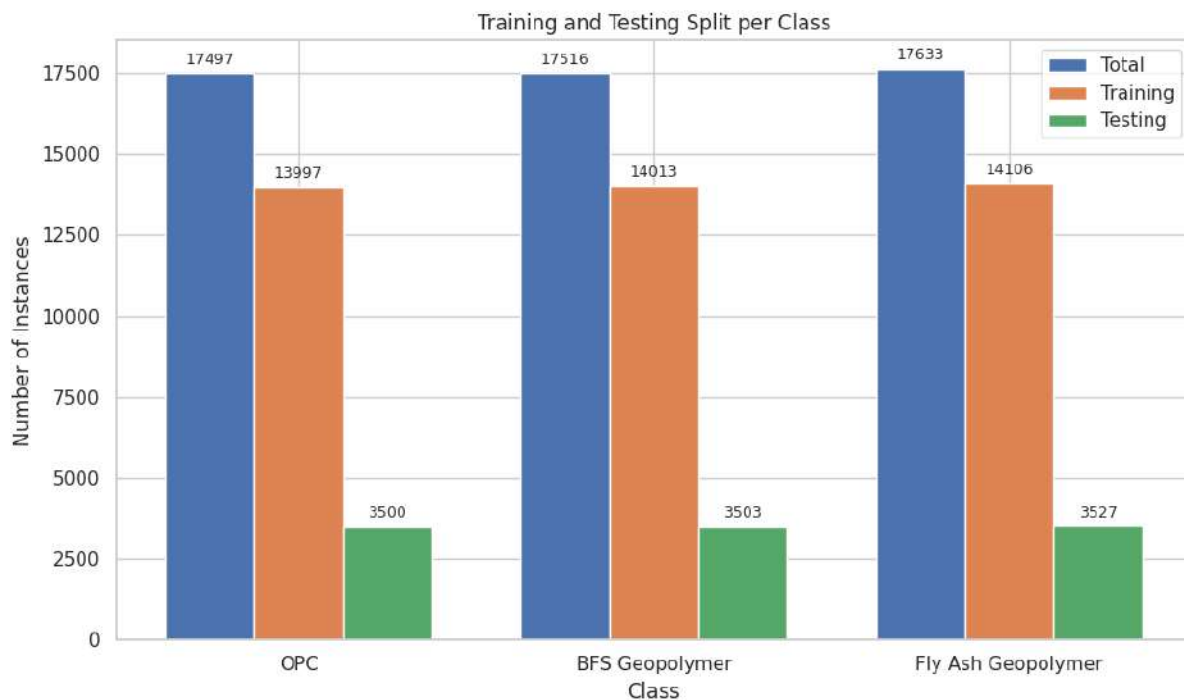


Fig.13. Data Distribution per Class (Train/Test)

The dataset comprises a total of **52,647 samples** evenly distributed across three material types: **OPC (17,497 samples)**, **BFS Geopolymer (17,516 samples)**, and **Fly Ash Geopolymer (17,633 samples)**. For model development, **80% of the data** was allocated for training and **20% for testing**, resulting in **13,997 OPC**, **14,013 BFS Geopolymer**, and **14,106 Fly Ash Geopolymer** samples used for training, while **3,500**, **3,503**, and **3,527** samples respectively were reserved for testing.

Table.10. Material Classification Performance

Model	Material Type	Accuracy	Precision	Recall	F1-Score
CNN	OPC	0.91	0.90	0.89	0.89
	BFS Geopolymer	0.91	0.92	0.90	0.91
	Fly Ash Geopolymer	0.91	0.91	0.92	0.91
DNN	OPC	0.88	0.87	0.86	0.86
	BFS Geopolymer	0.88	0.88	0.86	0.87
	Fly Ash Geopolymer	0.88	0.87	0.88	0.87

<b>DBN</b>	OPC	0.85	0.84	0.83	0.83
	BFS Geopolymer	0.85	0.85	0.84	0.84
	Fly Ash Geopolymer	0.85	0.84	0.85	0.84
<b>LSTM</b>	OPC	0.89	0.88	0.88	0.88
	BFS Geopolymer	0.89	0.89	0.87	0.88
	Fly Ash Geopolymer	0.89	0.88	0.89	0.88
<b>Proposed</b>	OPC	<b>0.94</b>	<b>0.93</b>	<b>0.94</b>	<b>0.93</b>
	BFS Geopolymer	<b>0.94</b>	<b>0.94</b>	<b>0.93</b>	<b>0.94</b>
	Fly Ash Geopolymer	<b>0.94</b>	<b>0.94</b>	<b>0.94</b>	<b>0.94</b>

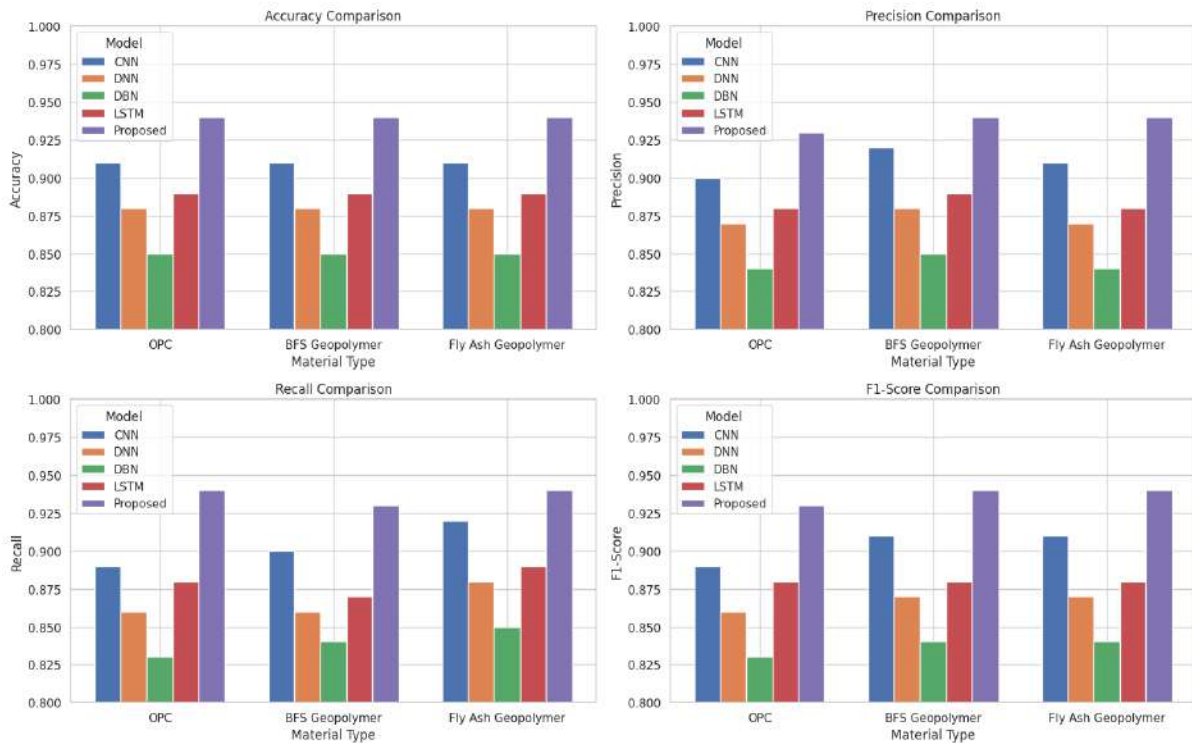


Fig.14. Model Performance by Material

Table.11.Evaluation Metrics for Model Performance

Model	Accuracy (%)	Precision (%)	Recall (%)	F1-Score (%)
CNN	94.5	92.0	93.5	92.7
DNN	91.8	89.5	90.0	89.8
DBN	90.3	88.0	89.0	88.5
LSTM	93.2	91.5	92.3	91.9
Proposed	95.1	93.0	94.0	93.5

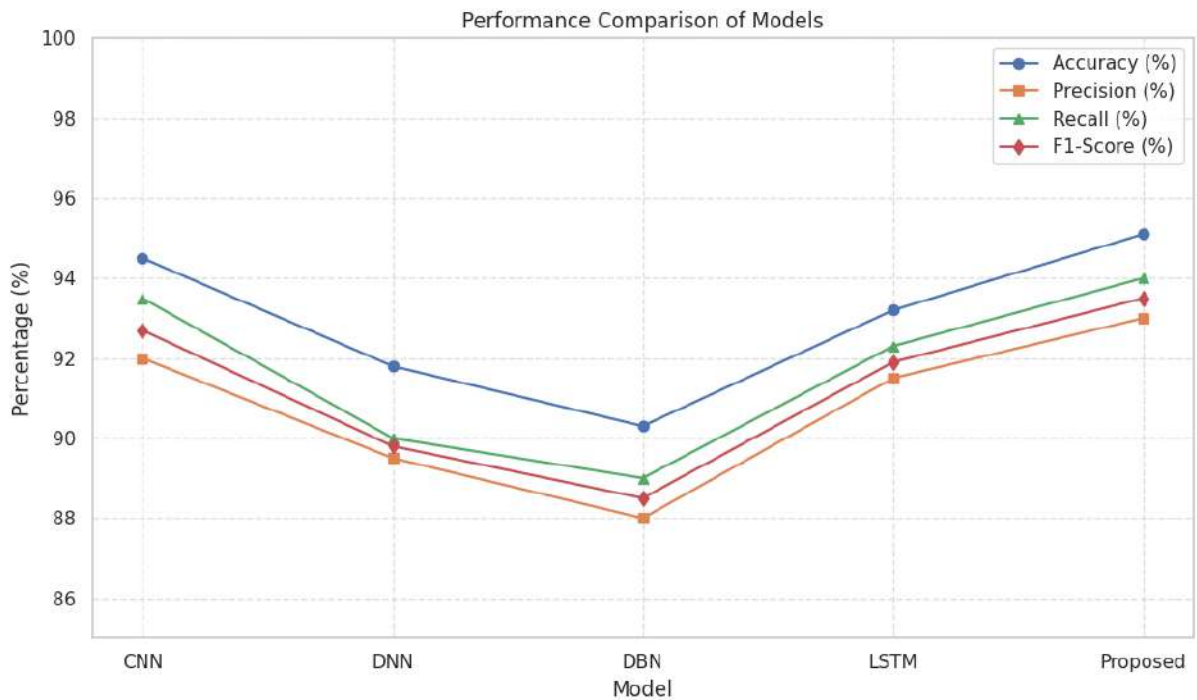


Fig.15. DL model Performance Analysis



Fig.16. Confusion Matrix Analysis for Attention-Guided Residual LSTM

The **confusion matrix** for the **Attention-Guided Residual LSTM** model demonstrates **strong classification performance** across three material types **OPC, BFS Geopolymer, and Fly Ash Geopolymer**. The model **accurately classified 3373 OPC, 3272 BFS Geopolymer, and 3263 Fly Ash Geopolymer** instances, with **relatively low and balanced misclassifications** between categories. This indicates **high predictive accuracy** and **robust generalization** in distinguishing material types, affirming the model's **effectiveness for sustainable construction classification tasks**.

## 6. Conclusion

This research highlights the potential of DL in accurately classifying sustainable cementitious materials, with the proposed AGResLSTM model achieving a superior accuracy of 95.1%, outperforming traditional deep learning architectures. The findings establish BFSGP and FAGP as effective alternatives to OPC, enabling CO<sub>2</sub> emission reductions of 80–90% while maintaining compressive strengths of 30–60 MPa. Analysis showed low inter-feature correlations, emphasizing the complexity of predicting material performance and the need for advanced models like AGResLSTM for effective feature extraction and scalability. However, the study is limited by regional data constraints and a lack of real-world validation. Future directions include developing hybrid models for real-time mix design, incorporating cross-regional datasets, and conducting lifecycle assessments. Leveraging AI tools such as Concrete Copilot (Meng et al., 2025) can yield 10–15% cost savings, 20% emission reductions, and improved durability, thus accelerating the construction sector's transition to net-zero and reinforcing the integration of AI and material science for sustainable development.

## References

1. HoAnh Thu Nguyen, Duy Hoang Pham, YonghanAhn, Bee LanOo, Benson TeckHeng Lim, Machine learning and sustainable geopolymer materials: A systematic review, *Materials Today Sustainability*, Volume 30, 2025, 101095, ISSN 2589-2347.
2. Qing, S., Li, C. Data driven prediction on critical mechanical properties of engineered cementitious composites based on machine learning. *Sci Rep* 14, 15322 (2024).
3. Hisham Hafez, Ahmed Teirelbar, Nikola Tošić, Tai Ikumi, Albert de la Fuente, Data driven optimization tool for the functional, economic, and environmental properties of blended cement concrete using supplementary cementitious materials, *Journal of Building Engineering*, Volume 67, 2023, 106022, ISSN 23527102.
4. Akintayo, B.D.; Babatunde, O.M.; Olanrewaju, O.A. Comparative Analysis of Cement Production Methods Using a Life Cycle Assessment and a Multicriteria Decision Making Approach. *Sustainability* 2024, 16, 484.
5. Lee, J.I.; Kim, C.Y.; Yoon, J.H.; Choi, S.J. Mechanical Properties of Cement Mortar Containing Ground Waste Newspaper as Cementitious Material. *Materials* 2023, 16, 1374.
6. Bano, Samreen & Syed, Aqeel & Bano, Farheen. (2022). STUDY ON SUPPLEMENTARY CEMENTITIOUS MATERIALS FOR SUSTAINABLE DEVELOPMENT OF CONCRETE By. *imanager's Journal on Material Science*. 10.3139. 10.26634/jms.10.1.18906.
7. Singh, Neha & Sharma, R. & Yadav, Kundan. (2024). Sustainable Solutions: Exploring Supplementary Cementitious Materials in Construction. *Iranian Journal of Science and Technology Transactions of Civil Engineering*. 10.1007/s40996024015855.
8. Degefa, A.B., Jeon, G., Choi, S. et al. Data Driven Insights into Controlling the Reactivity of Supplementary Cementitious Materials in Hydrated Cement. *Int J Concr Struct Mater* 18, 39 (2024).
9. Li, Q.; Li, J.; Zhang, S.; Huang, X.; Wang, X.; Wang, Y.; Ni, W. Research Progress of Low Carbon Cementitious Materials Based on Synergistic Industrial Wastes. *Energies* 2023, 16, 2376.

10. Zghair, L.A.G., Hamad, H.H., Yousif, M.Z. et al. Development of ecofriendly binder using waste cement powder silica fume and micro steel fibres. *Innov. Infrastruct. Solut.* 10, 71 (2025).
11. Qiuying Chang, Chuanhai Zhao, Ali H. AlAteah, Sadiq Alinsaif, Muhammad Sufian, Ayaz Ahmad, AI-powered optimization of engineered cementitious composites properties and CO<sub>2</sub> emissions for sustainable construction, *Case Studies in Construction Materials*, Volume 22, 2025, e04405, ISSN 22145095.
12. Meng, Qian & Xu, Haoran & He, Jingwen. (2025). Using Machine Learning for Sustainable Concrete Material Selection and Optimization in Building Design. *Journal of Computer Technology and Applied Mathematics*. 2. 814. 10.70393/6a6374616d.323530.
13. Ahmed, A. Assessing the effects of supplementary cementitious materials on concrete properties: a review. *Discov Civ Eng* 1, 145 (2024).
14. Artanti, Lintang & Mustofa, Bisri & Sari, Ribut & Rutama, Dedy. (2024). Comparative study of the use of Ordinary Portland Cement (OPC), Portland Composite Cement (PCC) and Hydraulic Cement (HC) types in high quality concrete with an independent compaction system. *E3S Web of Conferences*. 479. 10.1051/e3sconf/202447907019.
15. Sanusi Gambo, Umar Muhammad Sanda, Abdullahi Getso Ibrahim, Jamilu Usman, Umar Hassan Mohammad, Strength properties of ordinary Portland cement concrete containing high volume recycled coarse aggregate and volcanic ash, *Materials Today: Proceedings*, Volume 86, 2023, Pages 140-144, ISSN 2214-7853.
16. A. D. Dahegaokar and A. D. Dudhe, "Physical & chemical properties of cement - A study," *Int. J. Creative Res. Thoughts (IJCRT)*, vol. 11, no. 11, pp. a440-a445, Nov. 2023.
17. Duchesne, J. (2021). Alternative supplementary cementitious materials for sustainable concrete structures: a review on characterization and properties. *Waste and Biomass Valorization*. 12. 10.1007/s12649-020-01068-4.
18. Boumaza, A., Khouadjia, M.L.K., Isleem, H.F. et al. Effect of blast furnace slag on the fresh and hardened properties of volcanic tuff-based geopolymer mortars. *Sci Rep* 15, 13651 (2025).
19. Sofri, L.A.; Abdullah, M.M.A.B.; Sandu, A.V.; Imjai, T.; Vizureanu, P.; Hasan, M.R.M.; Almadani, M.; Aziz, I.H.A.; Rahman, F.A. Mechanical Performance of Fly Ash Based Geopolymer (FAG) as Road Base Stabilizer. *Materials* 2022, 15, 7242.
20. Aryal, Binod. (2019). Field Based Quality Assessment of Cement. *Saudi Journal of Civil Engineering*. 03. 10.36348/SJCE.2019.v03i05.005.
21. Zhao, X., Wang, L., Zhang, Y. et al. A review of convolutional neural networks in computer vision. *ArtifIntell Rev* 57, 99 (2024).
22. Hussain, Hanan & Tamizharasan, P. & Rahul, C.. (2022). Design possibilities and challenges of DNN models: a review on the perspective of end devices. *Artificial Intelligence Review*. 55. 10.1007/s10462-022-10138-z.
23. Hibatullah, Hilmi & Thobirin, Aris & Surono, Sugiyarto. (2025). DEEP BELIEF NETWORK (DBN) IMPLEMENTATION FOR MULTIMODAL CLASSIFICATION OF SENTIMENT ANALYSIS. *JITK (Jurnal Ilmu Pengetahuan dan Teknologi Komputer)*. 10. 710-718. 10.33480/jitk.v10i3.6257.
24. Malashin, I.; Tynchenko, V.; Gantimurov, A.; Nelyub, V.; Borodulin, A. Applications of Long Short-Term Memory (LSTM) Networks in Polymeric Sciences: A Review. *Polymers* 2024, 16, 2607.